

Spectrum of Photons Emitted in Coincidence with Fission of ^{235}U by Thermal Neutrons*

R. W. Peelle and F. C. Maienschein†

Oak Ridge National Laboratory, Oak Ridge, Tennessee 37830‡

(Received 23 September 1970)

The absolute energy spectrum of prompt photons emitted from the fission of ^{235}U by thermal neutrons was measured in the range from 0.01 to 10 MeV by using single-crystal, Compton, and pair NaI(Tl) scintillation spectrometers. Each was operated in ≈ 69 -nsec coincidence with a fission chamber exposed to thermal neutrons from a reactor. The pulse-height response functions of the spectrometers were constructed in detail by exposing the spectrometers to radioactive sources of known disintegration rates. These data were used to "unfold" the measured pulse-height spectra to give the absolute differential energy spectrum and its random uncertainties. A careful analysis of systematic uncertainties was also performed. The average number of photons per fission is 8.13 ± 0.35 and the average photon energy release per fission is 7.25 ± 0.26 MeV, both over the energy region from 10 keV to 10.5 MeV. The results obtained here are in approximate agreement with the recent measurement by Verbinski and Sund in the energy region above 140 keV. From 1.5 to 4 MeV the calculation of Zommer, Savel'er, and Prokofiev gives results which are close to the measurements. The observed total energy release in photon emission per fission has been predicted by two published calculations which treated statistical evaporation theory in different ways to enhance the emission of photons. The *K*-shell x-ray intensities for the light- and heavy-fragment groups were found to be 0.08 ± 0.02 and 0.23 ± 0.02 photons/fission, respectively. The x-ray intensities are consistent with internal conversion of the observed γ -ray spectrum for various assumed mixtures of *E1*, *E2*, and *M2* transitions, including roughly equal *E1*-*E2* mixtures; the intensities are not consistent with all the transitions having any single multipolarity.

I. INTRODUCTION

About one half of the photon energy release associated with fission is emitted just after prompt neutron emission. All observations of the prompt photon spectrum have shown a roughly exponential shape with a much greater fraction of low-energy transitions than is observed in neutron capture; this characteristic shape has been ascribed to the estimated high typical spin of the primary fragments.¹⁻³ The shape is also affected by the spread of fragment excitation energies preceding photon emission.

The decay periods of the prompt transitions have been studied by observing the distances free-flying fragments travel before photon emission, either by use of thin-slit collimators or by the presence of Doppler shift in discrete lines observed in geometries for which the length of fragment flight was known. Two measurements based on the first method have established an over-all dominant decay period in the range 0.01 to 0.05 nsec.^{1,4} Observations of many enhanced *E2* decays within the ground-state rotational bands of the more likely even-even fragments have shown lifetimes ≈ 1 nsec using the second method.⁵

Not all the photon emission associated with fission follows promptly after fragment separation. No direct evidence has been found for photon emission before fission, but at least two possible mech-

anisms have been proposed. Photon transitions following neutron capture could excite shape isomers decaying by spontaneous fission; this process could give photon emission preceding fission by an observable decay period in perhaps (0.01 to 0.1)% of all neutron captures. However, recent (*d, p*) experiments of Wolf *et al.*⁶ suggest that ~ 0.1 - μsec $^{236}\text{U}^*$ may decay largely by photon emission. The (*n, γf*) process of Stavinski and Shaker⁷ and of Lynn⁸ does not invoke shape isomerism and could give perhaps 10^{-3} of the prompt photon energy before the saddle point is reached. [The (*n, γf*) process could help explain the apparent minimum fission width of resonances observed in $^{235}\text{U}(n, f)$ reactions.] In the decay-time range of tens of nanoseconds through hundreds of microseconds, photon emission arises from isomeric transitions in the fragments.⁹⁻¹² The energy emitted in the isomeric transitions is a few (<5) percent of the total if the definition of "prompt" in the experimenter's apparatus is similar to that used here. Finally, for times of the order of 1 sec and longer, successive β decays of the fragments lead to the "fission product" γ rays.¹³

The absolute spectrum of photons emitted promptly after the fission of ^{235}U by thermal neutrons is reported here for the broad energy range from 0.01 to 10 MeV. For the utilized spectrometer systems, "prompt" was defined by coincidence resolving times in the range 55 to 69 nsec. Emphasis

was placed on the absolute yield and on careful error analyses, since isolated lines in the spectrum corresponding to lifetimes $\lesssim 10^{-10}$ sec would in any event be broadened by up to 4% by the motion of the emitting fission fragments in the nearly isotropic geometry used (with respect to the direction of fragment motion). Preliminary results, based on part of the data examined here, were published much earlier and summed to 7.2 ± 0.8 MeV/fission for photon energies above 0.3 MeV.¹² Gamble and Francis¹⁴ had earlier given a spectrum and a total energy release of 7.5 MeV; their single-crystal scintillation spectrometer was too large to avoid serious backgrounds from fission neutrons but too small to allow a high photofraction for γ rays above 1 MeV. Rau¹⁵ has more recently measured the spectrum between 0.1 and 2.5 MeV using a single-crystal spectrometer, and estimated a total energy release of 9.5 ± 0.23 MeV for energies above 0.1 MeV by combining his results with our preliminary results at the higher energies. In Sec. IV the present results are compared with those of Verbinski and Sund.¹⁶ A number of experiments have studied x-ray emission from the fission fragments; these works are cited in Sec. IV. The spectrum of prompt photons from ²⁵²Cf is similar to that for ²³⁵U.¹⁶⁻¹⁸ Information on the fragment-angle and mass-ratio correlations of the photon production may be found in the review papers of Johansson and Kleinheinz¹ and of Maier-Leibnitz *et al.*²

Only Zommer, Savel'ev, and Prokofiev¹⁹ (ZSP) have published a prediction of the spectrum of prompt γ rays. The total energy release in prompt photons has been estimated by averaging over the ensemble of predicted post-neutron fragments and excitation energies. Until recently the neutron evaporation process was assumed to preempt photon deexcitation whenever the former is energetically possible, and the corresponding estimated total photon energies were systematically low.²⁰⁻²² Thomas and Grover²³ have shown that, if photon emission is allowed to compete with low-energy neutron evaporation, the estimated energy release can reach the necessary ~ 7.5 MeV. In their Monte Carlo study of fragment deexcitation, Gordon and Aras²⁴ obtained a total photon energy release consistent with experiment. In their work the pairing-energy correction to the decay energy prevented evaporation of neutrons from most fragments having excitation energies just over the neutron-emission threshold.

The essential features of the subject experiment and its results are condensed into the sections below. A laboratory report²⁵ is available which gives complete details and tabulated results, and a brief note has been published giving an approximate fit

to the spectrum and tables of intensities observed within rather broad energy intervals.²⁶

II. OBTAINING THE PULSE-HEIGHT SPECTRUM

Two well-shielded spectrometer systems were used; each was operated in coincidence with pulses from an ionization chamber containing ²³⁵U placed in a beam of thermal neutrons from a reactor.

A. Neutron Beam and Fission Chamber Configurations

For energies above 0.4 MeV, multiple-crystal scintillation spectrometers²⁷ were used to provide high peak/total ratios in the pulse-height distributions for γ -ray energies up to 8 MeV. A variable high-intensity flux of thermal neutrons (up to 7×10^7 cm⁻² sec⁻¹) was incident on the spectrometer of Fig. 1 from the thermal column of the Bulk Shielding Reactor.²⁸ All spectrometer calibrations were obtained in this same geometry.

For energies below ~ 0.8 MeV, the single-crystal

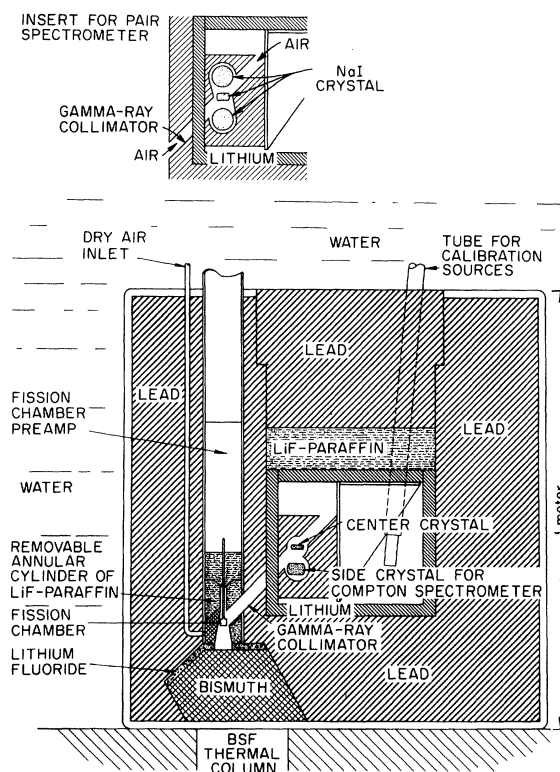


FIG. 1. Apparatus for high-energy measurements (side view). The Compton spectrometer is shown in place, while the pair spectrometer is shown in the insert. The poor collimation of the "beam" from the "thermal column" required the widespread use of lithium shielding to suppress production of capture γ rays.

scintillation spectrometer of Fig. 2 was utilized. A well-collimated $10^6\text{-cm}^{-2}\text{sec}^{-1}$ neutron beam passed through the fission chamber from the reflector of the Oak Ridge Graphite Reactor. Counts induced by fission neutrons were rejected by the neutron drift time along the 3.4-m He-filled γ -ray collimator. To allow observation of γ rays with energies as low as 10 keV, the surface density (115 mg/cm^2) of materials between the fission chamber and the scintillator was minimized and carefully determined to allow absorption corrections.

Table I lists the properties of the spiral-wound fission chamber²⁹ used at higher energies and the parallel plate chamber used at lower energies. In both cases a cascode-input preamplifier³⁰ was mounted a few centimeters from the chamber, feeding a DD-2 linear amplifier³¹ which drove a crossover pickoff timing circuit.³²

The angular correlation between the fission fragments and the γ -ray emission is anisotropic by as much as $\pm 7\%$.^{3,33} The parallel-plate ion chamber discriminated against fragments emitted nearly at right angles to the direction of observation; we estimate that as a result our raw observed yield was too high by $1 \pm 1\%$. The geometry of the spiral-wound chamber inhibited bias from this effect.

B. γ -Ray Spectrometers

Table I includes details on the individual scintillation counters, and for each spectrometer system gives the relation between the energy E (MeV) of a photon source and the position F (MeV) of the prominent peak in the corresponding pulse-height distribution. In each case the scale for F was calibrated using photopeaks observed in the "center" crystal alone.

Similar groups or channels of electronic instrumentation were attached to each detector. On each channel DD-2 linear amplifiers³¹ drove crossover timing units.³² Pulses from the directly-irradiated "center" crystal were sorted in a 256-channel pulse-height analyzer³⁴ triggered by appropriate coincidence conditions. A two-level coincidence circuit permitted use of broad-window differential pulse-height selection as shown in Table I on the "side" channels, B and C , together with 50–70-nsec resolving time. Considerable monitoring equipment was employed to aid lineup and stability checks.

Frequent linearity tests were performed. Conversion gains (ch/MeV), analyzer "zero," amplitude-dependent timing "walk," and coincidence circuit delays and resolving times were checked each day.

The efficiencies of complex spectrometer sys-

tems can drift from either geometric or electronic shifts. Daily efficiency measurements at 2.75 MeV during the high- and low-gain pair spectrometer runs showed 2.3 and 4% rms fluctuations, respectively, largely explained by known statistical variation in source-strength standardization and in the number of observed counts. The observed rms fluctuation in Compton-spectrometer observations on 1.27-MeV γ rays was 4%, compared with the 3% expected on the basis of counting uncertainties. For the single-crystal spectrometer, internal consistency was established within the set of fission data runs.

C. Combination of Pulse-Height Spectra

Conversion was made from the measured channel number, c , as recorded by the pulse-height analyzer, to energy units, p in MeV, by the equation: $p = [c - Q + \Delta c(c) + \delta c(p)]/h$, where h is the gain in channels/MeV, Q is the zero offset in channels, and Δc and δc are the analyzer and NaI(Tl) nonlinearity corrections in channels. (The correction δc was obtained from a zero-order approximation to p .) The gain and the zero offset were determined by exposure of the spectrometer to monoenergetic γ rays. The 0.4% gain uncertainty included drift. The values of the correction for analyzer

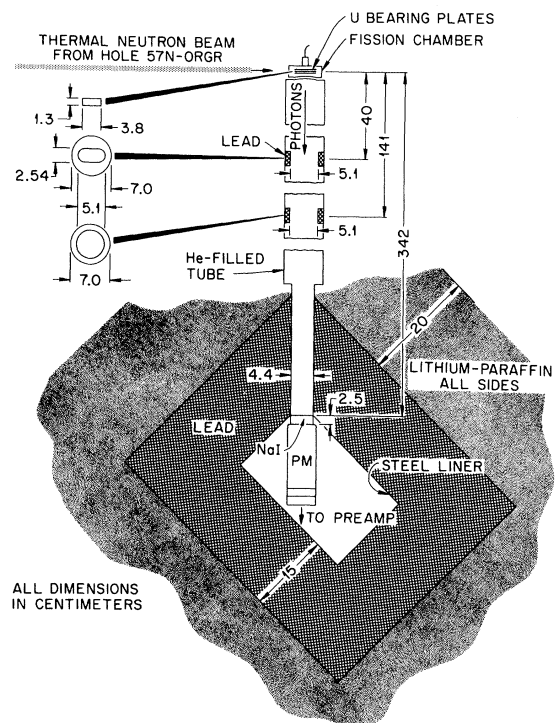


FIG. 2. Apparatus for low-energy measurements (top view).

nonlinearity were based on a distributed series of tests using a uniform pulse-height distribution from a special pulser. As corrected, the pulse-height scale was linear within 0.2%. The effects of scintillator nonlinearity³⁵ were absorbed into the zero offset, except that the low-energy data at 630 ch/MeV required an explicit correction as a function of pulse height.

In the combination of pulse-height spectra from many "runs" of up to one day each, counts were grouped into pulse-height bins of graduated width to reduce the numerical difficulty of the unfolding problem and yet retain most of the inherent energy resolution of each spectrometer. The bin width, B (in MeV) for the i th pulse-height bin was taken as $B_i = qp_i^{1/2}$, where p_i is the pulse height at the lower bin edge in MeV, and values of q are given in Table I.

D. Background Corrections

Neutron Effects

The flight-time discrimination against neutron-induced background in the spectrometer of Fig. 2 was tested by absorption measurements and by observing the counting rate in the NaI(Tl) counter vs delay time using a 21.5-nsec resolving time. A

broad peak 150 nsec after the prompt γ rays was fit in shape by converting the spectrum of fission neutrons to a time scale appropriate to the 3.4-m flight path.³⁶

The small size of the center crystals in the pair and Compton spectrometers reduced the relative effect of fission neutrons. After careful empirical improvements to the shielding in the spectrometer of Fig. 1, attenuation measurements in poor geometry were made with lead and polyethylene plugs in the collimator of the Compton spectrometer.³⁷ The results were consistent with any structureless neutron-induced background in the range 0–15%. To test more critically, a delayed coincidence measurement was made with the center crystal of the Compton spectrometer moved back to ~ 49 cm from the fission chamber. The time dependence of the results implied a $(4 \pm 4)\%$ neutron effect in the singles spectrum for the normal timing. The coincidence and side-channel pulse-height requirements of the spectrometers further reduced neutron effects.

To symmetrize the uncertainties from neutron effects and from fission-fragment anisotropy (Sec. II B), all pulse-height spectra were multiplied by 0.985. Table I lists the uncertainties from these effects in the uncompensated and com-

TABLE I. Properties of the three spectrometer systems.

	Single crystal	Compton	Pair
Energy range (MeV)	0.01 to 0.8	0.4 to 2.4	1.6 to 10.5
Fission rate (sec ⁻¹)	2.4×10^4	$\sim 3.3 \times 10^4$	$\sim 9 \times 10^4$
Mass of ²³⁵ U (g)	0.019	0.23	0.23
Volume containing sample	$1 \times 1.33 \times 3.8$ cm	1 \times 1-cm cylinder	
Governing resolution time (nsec)	69 ± 1	56 ± 1.5	56.4 ± 2.3
Peak position F	E	$\sim (E^2 - 0.0038 \text{ MeV}^2) / (E + 0.324 \text{ MeV})^a$	$E - (1.022 \text{ MeV})$
Scintillator size (cm)	4.45 diam \times 2.54 high	~ 0.95 thick \times 2.2 \times 2.2 ^b	1.9 thick \times 2.5 \times 2.5 ^c
Multiplier phototube used	Dumont 6292	Dumont 6291 ^b	Dumont 6291 ^c
Raw gain (channels/MeV) ($\pm 0.4\%$)	263, 630, and 2400	56	24 and 50
Total exposure time (h)	658	124	685
Bin width constant q (MeV ^{1/2}) ($B = qp^{1/2}$)	0.025	0.1	0.08 ^d
(Bin width)/(inherent FWHM)	~ 0.5	0.8	~ 1 ^e
Uncompensated uncertainty from photon anisotropy	$+0\%$ -2%	0	0
Uncompensated uncertainty from neutron background	$+0\%$ -1%	$+0\%$ -4%	$+0\%$ -2%
Final ^f uncertainty from anisotropy plus neutron background	$\pm 1\%$	$(-0.5 \pm 2)\%$	$(+0.5 \pm 1)\%$

^a Determined empirically by repeated measurements using up to 18 photon sources of known energy. The uncertainty ranged from 0.3 to 0.5%.

^b The "side" crystal of the Compton spectrometer was $\sim 3.8 \times 3.8 \times 2.54$ cm thick, biased for the 0.15- to 0.40-MeV region. It was mounted on a Dumont 6292 multiplier phototube.

^c Annihilation quanta were detected in right equilateral cylinders with diameter 5.1 cm, biased to cover the pulse-height region from 0.42 to 0.60 MeV. These crystals were mounted on Dumont 6292 multiplier phototubes.

^d Below 5.3 MeV. The value was 0.16 for energies between 5.3 and 7 MeV. Above 7 MeV two broad bins were used.

^e Below 5.3 MeV.

^f After the pulse-height spectrum was multiplied by 0.985.

pensated pulse-height spectra.

Random-Coincidence Background

Accidental coincidences in time of signals from uncorrelated events in the various detectors were compensated taking into account that true background coincidences occurred between various pairs and triples of detectors. The relevant rates were determined daily. The single random-coincidence contribution at low energy ($A \times D$), the most important contribution ($AB \times D$) for the Compton spectrometer, and the three most important contributions ($ABC \times D$, $ACD \times B$, and $AC \times BD$) for the pair spectrometer were subtracted bin by bin on the basis of observed lower-order coincident pulse-height spectra. The less-important contributions were compensated by adjusting the magnitude of the dominant backgrounds. The combined random-coincidence background was kept below 15% of the foreground for γ -ray energies below ~ 3 MeV but grew to equal the foreground at ~ 6 MeV. The careful correction techniques held the uncertainty from this effect below 1% through 4 MeV.

E. Corrections for Counting Losses

The chosen fission rates were limited by the fractional rate of lost counts which could be tolerated in the fission-chamber channel. Two such rate-dependent losses and a rate-independent one are described below.

Singles's Losses

The rate of fission events was corrected for accidental overlap of pulses leading to a single count for two or more fissions. The observed dead time 0.90 ± 0.03 μ sec leads to a 0.3% uncertainty in the number of fissions for the maximum counting rate of 9.4×10^4 /sec.

Coincidence Losses

Crossover pickoff timing circuits require a fixed pulse shape, so pulse-overlap shape distortion produced timing shifts which implied significant coincidence losses. The magnitude of this spectrum-dependent effect was evaluated by mixing pulser signals into the linear system with the experimental signals. The amplitude dependence of the rate of loss of pulser events was observed by the use of coincidence gating. Worst-case coincidence losses were 27%, leading to a 2.2% uncertainty in the corrected results for a segment of the pair spectrometer results.

Coincidence Circuit Losses

Timing jitter inherent in the use of crossover pickoff timing led to coincidence efficiency appreciably less than unity for pulse heights under 50 keV even though the resolving time was made larger than for the higher-energy measurements. Based on observations³⁸ with the fission chamber and scintillator of Fig. 2, the coincidence efficiency dropped to 0.96 at 30 keV and 0.77 at 10 keV, with uncertainties of 1.7 and 5%, respectively.

III. ANALYSIS FOR THE PHOTON ENERGY SPECTRUM

A. Problem Definition

If $\Gamma(E)$ is the desired photon energy spectrum from fission, if C_k^s is the number of counts per fission observed in pulse-height bin k of spectrometer system s , and if S_k^s is the corresponding statistical uncertainty, the bin response function $R_k^s(E)$ is defined by

$$\int_E R_k^s(E) \Gamma(E) dE = \hat{C}_k^s \cong C_k^s \pm S_k^s, \quad (1)$$

where \hat{C}_k^s is the expectation value of the binned count C_k^s . The function $R_k^s(E)$ is the average probability that a fission γ ray of energy E will be counted in pulse-height bin k of spectrometer s . An "unfolding" procedure was required to estimate a range of photon spectral intensities consistent with the observed pulse-height distributions.

The pulse-height distributions observed for a series of photon energies E_i were fit in both energy (E) and pulse-height (p) variables using non-linear least-squares analyses. The functional forms of the responses $R^s(E, p)$ were chosen empirically. When the fitting was complete, the $R^s(E, p)$ were integrated over successive pulse-height bins to obtain the $R_k^s(E)$ defined above.

The dependence of efficiency on γ -ray energy was based upon the use of calibration sources of known intensity mounted in the same geometry as the fission chambers described in Sec. II.

B. Calibration of Source Strengths

Most of the source strengths were established using calibrated 4π -ionization chambers, but a few were determined directly by absolute counting procedures.

Ion Chamber Calibration

The two chambers used were 10-in. right circular hollow cylinders of iron, filled with 40 atm of argon and provided with reentrant tubes along

their symmetry axes to hold a source near the center. Ion currents were corrected for drift and ion recombination effects. The energy dependence of each chamber's efficiency was based on measurements of a series of sources, with energies up through 2.75 MeV, calibrated by absolute β - γ and γ - γ coincidence counting.³⁹⁻⁴² Scattering in the source capsules was compensated taking into account the chamber efficiency at the scattered energy. Final uncertainties on sources calibrated in this manner generally ranged from 1.5 to 3%. A memorandum completely describes our use of these chambers.⁴³

Direct Absolute Calibration

A ^{24}Na source was calibrated within 1%, using absolute γ - γ coincidence counting, several decay periods after it was used to calibrate the pair spectrometer at 2.75 MeV. (The uncertainty from the decay correction was small.) Our knowledge of the pair spectrometer efficiency above 3 MeV is dominated by an experiment which used the 4.4- and 11.8-MeV cascade of the $^{11}\text{B}(p, \gamma)^{12}\text{C}$ (200-keV protons) reaction. γ - γ absolute counting was performed during measurement of the pair spectrometer response. Angular distributions and correlations were accounted for in the analysis.⁴⁰ Long-term accelerator breakdown terminated the experiment and thereby forced a 5% uncertainty in the efficiency at 4.4 MeV.

Absorption of γ Rays

Corrections were entered to compensate for the differences between the absorption properties of the fission chambers and the calibration sources.

For the low-energy measurements with the single-crystal spectrometer, absorption by the uranium dominated; for energies below about 50 keV, uncertainties were introduced by imperfect knowledge of the thicknesses of the chamber plates and perhaps of the γ -ray cross sections.^{44, 45} The errors in the calculated photon transmissions were judged to be <1% for photon energies >50 keV, <4% for photon energies >33 keV, and <20% for photon energies >10 keV.

For the pair and Compton spectrometers, the most frequently used sources were mixed with graphite and aluminum powder and placed in brass cans just like those for the fission chambers. The ratios of transmissions for the fission chamber and the sources differed from unity by ~10% in the worst cases, and are all known to within 1%.

C. Fitting the Observed Spectrometer Response

For each spectrometer system (s), an attempt

was made to find parameters d_{ij} to represent within experimental uncertainty the response $R^s(E, p)$ as a function of γ -ray energy (E) and pulse height (p). Calibration spectra (up to 45 cases for each s) were fitted in terms of 9-11 parameters $P_i(E_k)$ for each source energy,⁴⁶ and then the variation of these parameters with γ -ray energy was fitted in a separate procedure by adjusting the d_{ij} .

Correlations among the P_i parameters were utilized in performing fits as a function of γ -ray energy by employing a nondiagonal weighting matrix obtained as the inverse of the variance matrix of the P_i .

The detailed form of the response function for each of the three spectrometers is given explicitly in Ref. 25. The general form adopted for the response function was

$$R(E, p) = (\text{peak efficiency}) \\ \times [(\text{unit-area Gaussian for the peak shape}) \\ + (\text{tail magnitude})(\text{tail shape}) \\ + (\text{other localized contributions})]. \quad (2)$$

Typically, the tail shapes were combinations of exponential terms, while the energy-localized contributions were normal density functions.

The energy dependence of the peak efficiency of the pair spectrometer is shown in Fig. 3(a) divided by the Hough formulation⁴⁷ of the Born approximation to the pair cross section. The quotient decreases with increasing γ -ray energy because of the escape of radiations from the central crystal and because of positron annihilation in flight. A calculation³⁹ based on the experimental data in Fig. 3(a) gave values of the pair cross section in NaI which were consistent with published data^{45, 48} and had comparable estimated uncertainties.

The peak efficiency for the Compton spectrometer is shown in Fig. 3(b). The efficiency drops rapidly below ~300 keV because of reduced probability of escape of the backscattered photon from the center crystal. For the single-crystal spectrometer peak efficiency, shown in Fig. 3(c), the low-energy falloff is due to absorption in the fission chamber and spectrometer system.

The energy resolution or width of the full-energy peak increased smoothly with energy for all spectrometers. The window functions shown later give an idea of this variation.

The relative tail magnitude and the most important tail shape parameters showed a smooth variation with γ -ray energy. No problems with nonunique least-squares fits were encountered, once plausible forms were developed for the response functions.

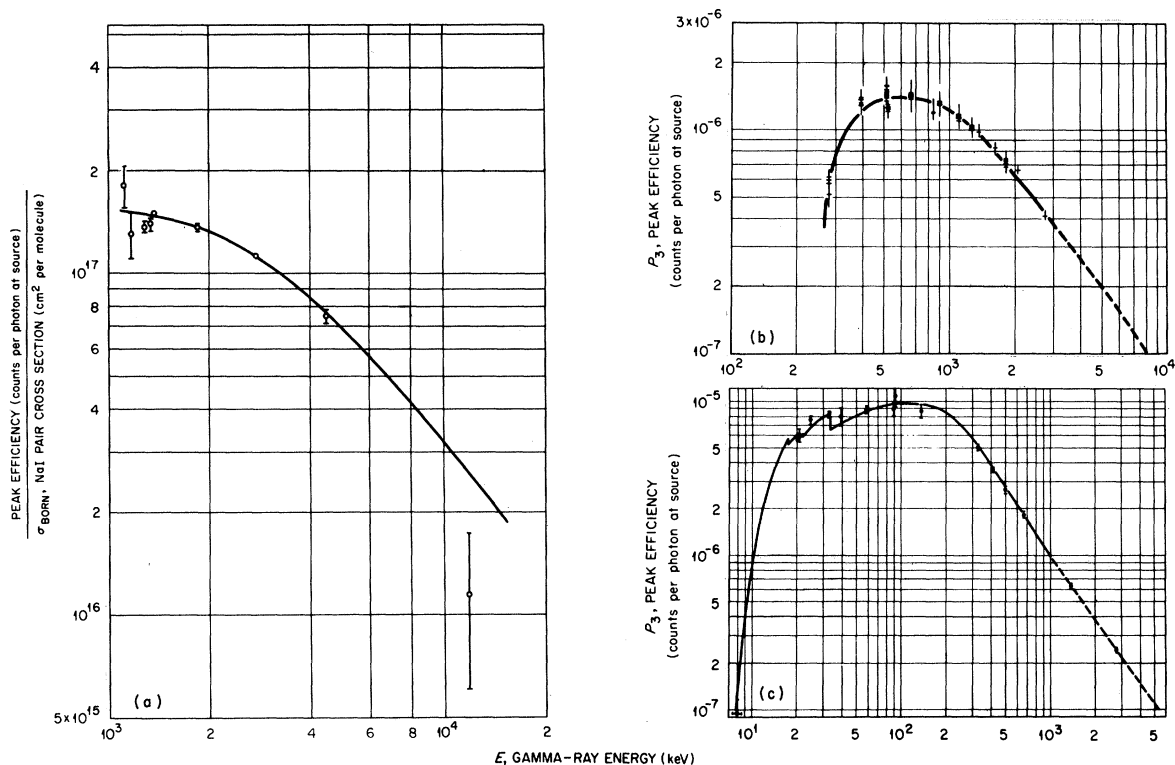


FIG. 3. The energy dependence of the peak efficiencies of the spectrometer systems. The peak efficiencies are defined per photon emitted from an isotropic source located at the center of the fission chamber and include self-absorption in the apparatus. (a) The peak efficiency of the pair spectrometer, divided by the Born approximation to the pair-production cross section of NaI in $\text{cm}^2/\text{molecule}$. The line was drawn to connect the points. (b) The peak efficiency of the Compton spectrometer. The horizontal bars on the points refer to individual efficiency measurements. The solid line is a fit to the points. The extrapolation above 3 MeV was based on the cross section for the Compton effect and an estimate of electron escape from the crystal. (c) The peak efficiency of the single-crystal spectrometer. The points represent the weighted averages of several measurements. The calculated solid curve is based on total efficiencies based on NaI cross sections, on peak/total ratios of Lazar [W. W. Mott and R. B. Sutton, in *Handbuch der Physik*, edited by S. Flügge (Springer-Verlag, Berlin, Germany, 1958), Vol. XLV, p. 124], the iodine escape fractions of Axel [P. Axel, *Rev. Sci. Instr.* **25**, 391 (1954)], and self-absorption calculations for intervening materials. The dashed extrapolation above 1 MeV is drawn to pass through the experimental points.

Figure 4 compares experimental calibration spectra for individual sources with pulse-height distributions generated from the $R(E, p)$ functions. The peak of the pair spectrometer response is well defined at least for incident energies through 7 MeV, but deteriorates by 10.8 MeV. The Compton spectrometer was not utilized for energies as high as the 2.75-MeV case illustrated in 4(b).

D. Unfolding Analysis

At the input to the spectrum "unfolding" problem, there were experimental counts, uncertainties, and bin response functions for 129 data bins. We needed to estimate both the γ -ray spectrum $\Gamma(E)$ over the whole energy range and integrals of this spectrum over broad energy regions. The energy resolution for the output spectrum was set

equal to the energy resolution of the peaks in the bin response functions. The combined analysis for the three spectrometer systems was performed using a subset of the FERD method of Burrus.⁴⁹

All the quantities g_i for which we desired estimates are given by weighted integrals over the unknown underlying photon spectrum $\Gamma(E)$ of the form

$$g_i = \int_E w_i(E) \Gamma(E) dE. \quad (3)$$

$w_i(E)$ is an energy-dependent weighting function called a "window." For example, $w_i(E) = 1$ would be appropriate if g_i were to be the total number of emitted photons/fission; and $w_i(E) = G(E_0)$, a unit-area normal frequency function centered at E_0 , would approximate the number of photons fission⁻¹ MeV⁻¹ at E_0 , subject to the standard deviation of

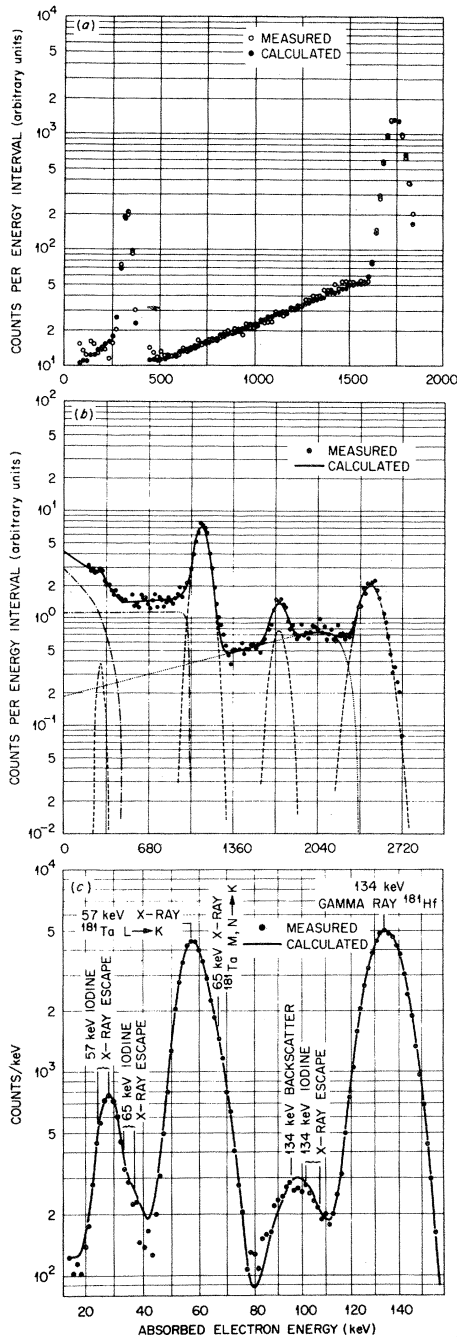


FIG. 4. Comparison of experimental calibration spectra with fitted response functions. (a)–(c), respectively, compare input data with fitted functions for a ^{24}Na source in the pair spectrometer, a ^{24}Na source in the Compton spectrometer, and a ^{181}Hf source in the single-crystal spectrometer. In (b) the fit is to these data alone, and the various features of the fitting function are shown separately. At lower photon energies the Compton spectrometer response is less complex. In (a) and in (c) interpolated parameters were used to generate the curves.

G. The FERD method of Burrus consists first in fitting each $w(E)$ with a combination of the response functions $\sum_k u_k R_k(E)$, a combination nearly optimized to minimize the over-all uncertainty in g when g is estimated as follows:

$$g = \int_E \Gamma(E) w(E) dE \cong \int_E \Gamma(E) [\sum_k u_k R_k(E)] dE \quad (4)$$

$$\cong \sum_k u_k \int_E \Gamma(E) R_k(E) dE \cong \sum_k u_k (C_k \pm S_k).$$

Equation (1) has been used in the last step. The u_k form the “combination vector.” The main task of the unfolding is to assign values to the u ’s for each window.

In forming the synthetic (fitted) window $\sum_k u_k R_k(E)$ to approximate the given $w(E)$, the FERD system takes into account the nonnegativity of $\Gamma(E)$ to minimize (approximately) the over-all uncertainty in g . Too close a fit between the synthetic and real windows may lead to successive u_k being large and of alternating sign, in turn leading to excessive statistical uncertainties in g just from propagation of the uncertainties in the binned counts C_k . On the other extreme, a poor match between imposed and synthetic windows may lead to a systematic error if it occurs at the same energy as a large spike in Γ . In FERD the latter problem is eliminated in a second step in which the combination vector \vec{u} is adjusted to obtain two vectors \vec{u}_{10} and \vec{u}_{up} , such that for every energy E they form upper and lower bounds on $w(E)$,

$$\sum_k u_{10,k} R_k(E) \leq w(E) \leq \sum_k u_{up,k} R_k(E). \quad (5)$$

Since $\Gamma(E)$ is taken as *a priori* nonnegative, the final confidence interval for g given by FERD has upper and lower ($\geq \frac{2}{3}$) confidence limits as follows:

$$g_{up} = \sum_k u_{up,k} C_k + (\sum_k u_k^2 S_k^2)^{1/2}, \quad (6)$$

$$g_{10} = \sum_k u_{10,k} C_k - (\sum_k u_k^2 S_k^2)^{1/2}.$$

This system for establishing the output confidence interval has the strength that if the user puts in a $w(E)$ which is an unreasonably sharp function of energy, he is rewarded with an honest if remarkably broad confidence interval. The FERD confidence limits are firm with respect to unscrambling difficulties; no iterative techniques are required.

The main representation of the output spectrum was based on a choice of 129 quasinnormal window functions which were formed by normalizing to unit area the “peak” section of each $R_k(E)$. The energy points in Figs. 5 and 6 are the mean energies of these numerically derived window functions.

In the numerical procedures, $w(E)$ and $R_k(E)$ were represented by their values at 369 "comparison energies" chosen so that at least three points were fixed within the region corresponding to each pulse-height bin. Experience, and a test with $\frac{5}{3}$ as many comparison energies, indicated the results to be stable relative to this mesh spacing.

IV. RESULTS AND DISCUSSION

A. γ -Ray Spectrum

The photon spectral yield per fission is shown in Figs. 5 and 6. To make small differences visible in Fig. 6, the abscissa are plotted on a square-root scale and ordinates have been multiplied by e^E , where E is in MeV. The illustrated confidence intervals include statistical uncertainties in the data and the difficulties the FERD program

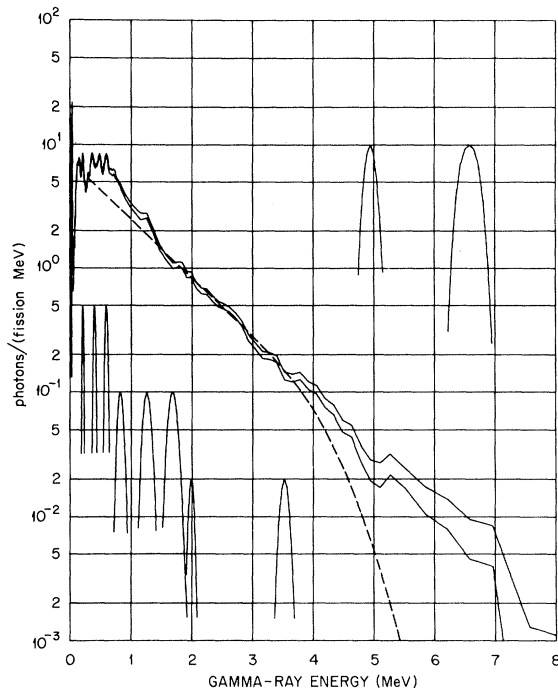


FIG. 5. The energy spectrum of photons emitted within 69 nsec after fission of ^{235}U induced by thermal neutrons (within 55 nsec for energies above 0.8 MeV). The two solid lines represent the two-thirds confidence limits to the experimental results if the systematic uncertainties of Fig. 7 are not considered. The confidence limits obtained from the unscrambling process for each window are plotted at its mean energy, and these points are joined by straight-line segments. The nearly normal shapes shown at the lower left and upper right are typical "windows" used in unscrambling the results. The windows were drawn as straight lines joining their amplitudes at successive comparison energies. The dashed line is the predicted (prompt) spectrum of ZSP (Ref. 19) based upon an application of statistical theory. (Values were extracted from the curve in the cited work.)

has in finding synthetic windows which remain above and below the input window functions. The intervals do not include the systematic uncertainties discussed in IV B. These figures include sets of typical window shapes; recall that window shapes determine the energy resolution available in the results. In Fig. 6, several peaks are apparent in the spectrum with widths comparable with the energy resolution. The lowest peaks at about 15.5 and 31.5 keV are properly placed to be K -shell x rays from the light and heavy fission fragments, respectively.

Spectrometer systems overlapped in the ranges 0.42–0.81 and 1.6–2.4 MeV. The plots represent the FERD confidence limits for quasinormal windows matching the resolution of the single-crystal spectrometer for energies up to 0.74 MeV, the Compton spectrometer for energies between 0.74 and 1.8 MeV, and the pair spectrometer for energies above 1.8 MeV. In the low-energy overlap region and above 1.8 MeV there is no disagreement between the results for the windows of different width. Below 1.7 MeV, the results from the narrower "pair" windows rise above the quoted values until at 1.6 MeV the mean values differ by about twice the linear sum of the quoted uncertainties. Count data for the entire overlap regions were retained and automatically weighted by FERD into the results. It was possible to broaden or narrow the breadth of the data overlap regions, and trial inclusions of less data did affect the answers in and near the overlap areas. These output instabilities appear to be covered by the systematic uncertainties discussed below.

In the pulse-height spectrum the ~ 15 -keV x-ray peak sits atop a background having about three times its area, while the 32-keV peak has an area equal to that of its apparent background. The results presented for the x-ray region (10 through 44 keV) were obtained using a count vector confined to this energy range and obtained by subtracting from the observed pulse spectrum an essentially flat spectrum which seems to have arisen from photons of higher energy. We assumed, in essence, that the two apparent peaks are from K x-ray emission from the light- and heavy-fragment groups and that no other processes give rise to photons in this energy range.⁵⁰ This treatment was chosen because otherwise the unscrambled photon spectrum did not suggest the lower edge of the 15-keV x-ray group which was so apparent in the raw data. The difficulty with the standard analysis occurred because our response functions are imperfectly known at extremely low pulse heights, and any errors in the 10-keV region are amplified by the quite low efficiency there.

The output strengths of the x-ray groups are

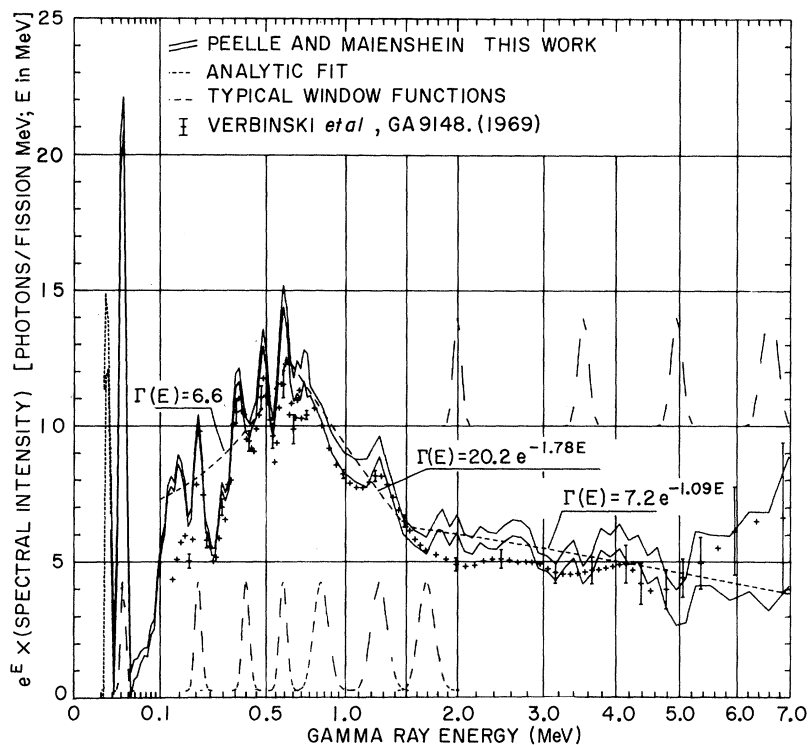


FIG. 6. Scaled spectra of prompt photons emitted following fission of ^{235}U induced by thermal neutrons. All spectral intensities have been multiplied by $e^{(E)}$ with E in MeV, and the abscissa has been stretched to fit an $(E)^{1/2}$ scale. The upper and lower confidence intervals from the present work have been joined by straight lines as in Fig. 4; for the dashed curve shown below 20 keV the uncertainty in the count vector did not include any contribution from the uncertainty in the background subtracted in the x-ray region. The confidence intervals do not include the systematic uncertainties of Fig. 7. Typical quasinormal window functions are shown as straight-line segments joining alternate pairs of comparison energies. The data of Verbinski and Sund (Ref. 16) are shown as + signs, with random uncertainties shown on some of the points; the systematic uncertainties for these data are not shown. The dashed curve corresponding to the labeled formulas is a fit further described in Ref. 26.

(0.08 ± 0.02) light-fragment and (0.23 ± 0.02) heavy-fragment K x rays per fission,⁵¹ giving respective photon energy releases per fission of 1.3 ± 0.3 and 7.4 ± 0.6 keV. These intensities were based both on the FERD outputs and on direct application of average efficiencies from Fig. 3(c) to the observed numbers of counts in the x-ray peaks. In estimating the efficiency and uncertainty for the heavy-fragment group, we judged that about 0.4 ± 0.2 of the heavy-fragment x rays are emitted with energies above the iodine K -absorption edge at 33.2 keV. This judgment accounts for $\frac{2}{3}$ the estimated uncertainty. (All the $K\beta$ lines for $z > 53$ are above this energy and 33.2 keV comes between the $K\alpha$ lines for $z = 57$.) If relative intensities are taken from the work of Bohn, Wehring, and Wyman,⁵² who observed only those transitions with decay periods ≤ 1 nsec, the fraction of x rays with energies over the absorption edge is about 0.3.

Above 0.7 MeV the spectrum in Figs. 5 and 6 is remarkably consistent with the earlier result¹²

based on part of the data treated here. Below 0.7 MeV the systematic errors in the preliminary analysis produced changes as large as expected.

Above 0.6 MeV the spectrum exhibits a rapid falloff with energy. Thirty percent of the emitted photons have energies above 1 MeV, and only 11% have energies above 1.8 MeV.

B. Systematic Uncertainties

Our systematic uncertainties are generally a function of photon energy, but they enter in the same sense through a broad energy region. We have assumed that the various systematic uncertainties are orthogonal and may be combined by summing the squared uncertainties. Figure 7 illustrates the over-all result of the analysis of systematic uncertainties. The best estimate of the full two-thirds confidence interval at any point in the spectrum can be obtained by combining the "total" value from Fig. 7 with the plotted uncertainty in Fig. 6.

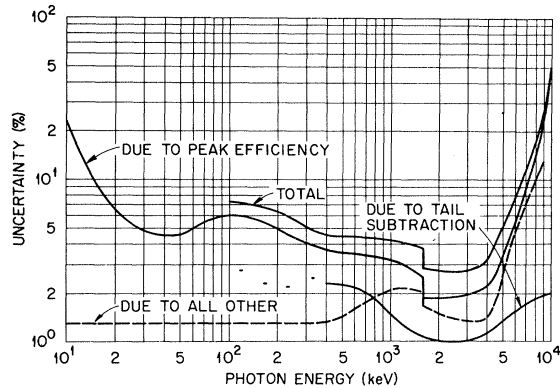


FIG. 7. Energy dependence of the systematic or correlated uncertainties in the prompt-fission photon spectrum. The various significant contributions are labeled on the graph. The discontinuity at 1.6 MeV arises because this is the lowest energy at which information from the pair spectrometer is used. The uncertainty due to tail subtraction is shown only at isolated points below 400 keV, since it is approximately constant at ~ 0.10 photons fission $^{-1}$ MeV $^{-1}$. (The percentage uncertainty fluctuates rapidly at low energies in accordance with the peaks and valleys of the γ -ray spectrum.)

The spectrometers were designed so that the relatively easily understood uncertainties in the peak efficiencies would give the largest contribution to the response function errors. Below 15 keV a large uncertainty is induced by difficulties in estimating or measuring the absorption of materials along the γ -ray flight path, while above 7 MeV the peak efficiency becomes poorly known because the pair spectrometer peak/total ratio was extrapolated into this region. Between these extremes three clues were utilized in estimating the value of the uncertainties: (a) the scatter in measured absolute peak efficiencies around the interpolating line used in the analysis; (b) the output covariance matrix from the least-squares interpolation procedure which used input data having uncertainties propagated from the observed pulse-height spectra; and (c) the sensitivity of the results to the size of the spectrometer overlap regions used. Generally, these clues implied the same uncertainty levels within a factor of 2; the

plotted values reflect a judicious compromise.

A complex systematic difficulty arises in the propagation of uncertainties in the "tail" response of each spectrometer. To allow an estimate of the resulting output uncertainties, we first obtained an energy-dependent relative uncertainty in the magnitude of each important feature of the spectrometer tail response functions. For each such feature a perturbed response matrix was then generated in which the area of that feature was increased by one standard error over the whole range of photon energies. The whole spectrum was then unscrambled using the perturbed matrix for that spectrometer and the normal matrix for the other two spectrometers. That feature's contribution to the over-all uncertainty was assessed by observing the resulting shifts in the output estimates. Below 1 MeV, tail-fraction effects were significant; below 400 keV, they were important; and below 70 keV, they became dominant. As expected, the most important tail uncertainty was the magnitude of the Compton continuum for the single-crystal spectrometer.

Uncertainty in the extent of uncompensated neutron background is discussed in Sec. II. In the restricted range from 0.8 to 1.8 MeV, it affects the over-all systematic uncertainty.

C. Integral γ -Ray Yields

The number of photons/fission and the MeV/fission emitted over the energy interval from 10 keV to 10.5 MeV within 69 nsec after fission (within 56 nsec for $E > 0.7$ MeV) were obtained using windows $w(E) = 1$ and E in FERD, and are shown in the first line of Table II. The quoted uncertainties are dominantly systematic in origin, and were estimated by weighting with the observed spectrum the uncertainties illustrated in Fig. 7. The energy yield per fission from photons below 10 keV and above 10.5 MeV should be negligible. The number of photons/fission below 10 keV probably does not exceed 0.1 (mostly L -shell x rays), and no photons are expected above 10.5 MeV. (See Sec. IV E, F for a discussion of the energy expected to be represented by conversion processes and by γ rays

TABLE II. Integral yields per fission of photons and of photon energy.

Energy range (MeV)	Photons/fission	MeV/Fission	Reference
0.010-10.5	8.13 ± 0.35	7.25 ± 0.26	This work
0.14-10.0	7.45 ± 0.32	7.18 ± 0.26	This work
0.14-10.0	6.69 ± 0.3	6.51 ± 0.3	16
0.1-10.0	7.95 ± 0.25	9.51 ± 0.23	15
0.1-7.6	7.5	7.5	14
0.3-10.5	7.4 ± 0.8	7.2 ± 0.8	12

from isomeric states.)

D. Comparison with Other Measurements

Figure 6 includes a comparison of our spectrum with the recent results of Verbinski and Sund¹⁶ for the energy range above 0.14 MeV. These authors used a large NaI scintillation spectrometer with an anticoincidence mantle to study photons produced within ~ 10 nsec of fission in samples of ^{235}U and ^{239}Pu by thermal neutrons from a reactor, and in ^{252}Cf (spontaneous fission). Time of flight was used to exclude neutron backgrounds. Their results agree rather well with ours, but disagreement appears in the average over the 1.7- to 2.8-MeV region. In the low-energy part of the spectrum, except at ~ 150 keV, the two spectra show nearly the same structure though the magnitudes differ. If the difference between the experimental results is real, it may arise from the shorter resolving time used by Verbinski and Sund. [Bridwell's results⁹ indicate substantial strength for decay periods longer than 10 nsec - presumably transitions of a few 100 keV (see Sec. IV E)].

Integral yields of photons per fission and the energy releases per fission are summarized in Table II. Our results are consistent within error with our preliminary analysis, but results of the final analysis reported here should be used. The yields of Verbinski and Sund¹⁶ are lower than ours, perhaps not significantly. Rau's photo energy release per fission appears quite high and his error assignment is surely too low. (See note with Ref. 15.)

Some idea of the detail in the low-energy part of the spectrum may be gained from the measurements of Horsch and Michaelis,⁵³ which were performed in a manner to allow reduction in Doppler broadening and identification of the mass of the emitting fragment. These fragment-dependent spectra show ~ 35 γ rays below 600 keV. The yields were not yet determined. Even taking into account our broader energy resolution, correlations with the Horsch spectra are evident to the eye only near 200 and 600 keV. Similar though more detailed work on ^{252}Cf fission has revealed a rich structure of ground-state rotational bands at least in the light even-even fragments, with ground-state transition intensities about equal to the corresponding independent radiochemical yields.⁵ Adjacent even-even nuclides tend to have about equal level spacings, so structurelike that observed in the gross spectrum is likely to arise in the average over the fragment ensemble.

E. X-Ray Yields

The study of x-ray yields is confused by their

time dependence relative to fission, since the experimental results cover a variety of time intervals. (In some cases the interval is determined by the length of the fragment flight path visible to the γ -ray detector.) Bridwell, Wyman, and Wehring,⁹ Glendenin, Unik, and Griffin,⁵⁴ and Thomas *et al.*⁵⁵ have demonstrated that the x rays predominantly have nuclear rather than atomic lifetimes, and so may be ascribed to deexcitation following internal conversion. Bridwell, Wyman, and Wehring, went further and attempted to fit the observed time dependence for the x rays from fission of ^{235}U with sums of three exponential "components" for the lighter- and heavier-fragment groups. X-ray intensities were measured for 80 nsec after fission for the light fragments and for 27 nsec for the heavy fragments. Thirty and 25% of the x rays from light and heavy fragments, respectively, had apparent periods of 75 and 30 nsec, and it was indicated that only $\sim \frac{1}{2}$ of the x rays appear to follow decay periods shorter than a few nanoseconds. The idea that substantial intensity exists into the 0.1- μ sec time region is qualitatively confirmed by studies of the isomeric γ -ray transitions in this time range,^{11, 12, 56} many of which are surely accompanied by internal conversion.

Table III summarizes the measurements of x-ray yields from light and heavy fragments from thermal-neutron fission of ^{235}U , along with the time period after fission included in the measurements. The yields are widely discrepant, but the time periods studied account for some of the variance. Our experiment suffered less from geometrical uncertainty than most, and included rather careful efficiency determinations in the relevant energy region; but had higher absorption for the light-fragment x rays than some of the other experiments. Most of the studies quoted in Table III concentrated on questions other than the absolute intensities.

If assumptions are made concerning the distribution of the γ -ray emitters among the fission fragments, the consistency between the x-ray intensity and that of the remainder of the spectrum can be checked if one is given the multipole order of the radiation. (Only the part of the γ -ray spectrum which has appreciable internal conversion coefficients, i.e., below ~ 0.4 MeV, affects the results.) Glendenin and Griffin⁵⁷ performed such a study by averaging over the charge distribution from fission of ^{252}Cf using their own x-ray measurements and the spectrum of Smith, Fields, and Friedman.¹⁷ They assumed an equal mixture of $E2$ and $M1$ transitions and were able to fit the intensity of their data satisfactorily by assuming that the emitted spectrum is the same for all fragments. The hazards are so great of this latter approximation and of

TABLE III. The yield of K-shell x rays from fission of ^{235}U induced by thermal neutrons.

Yield of K x rays per fission		Reference	Time limit (nsec)
From light fragments	From heavy fragments		
0.043 ± (0.011) ^a	0.12 ± (0.03) ^a	b	~1
0.07 ± .01	0.17 ± 0.02	52	~1
0.08 ± 0.02	0.23 ± 0.02	This work	68
0.12 ± 0.03	0.20 ± 0.05	c	~100 ^j
0.10 ± 0.03	...	d	200 ^a
...	0.42 ± 0.12	e	200
...	0.45 ± 0.15	f	200
0.13 ± 0.02	0.21 ± 0.03	g	200
0.17 ± 0.06	0.43 ± 0.04	9	300 ^j
0.18 ± 0.06	0.34 ± 0.09	h	350
0.08 ± 0.01	0.30 ± 0.02	i	600

^aValues estimated by us on the basis of the cited works.

^bL. E. Glendenin *et al.*, in *Proceedings of the Second International Atomic Energy Symposium on Physics and Chemistry of Fission, Vienna, Austria, 1969* (International Atomic Energy Agency, Vienna, Austria, 1969), p. 781.

^cB. W. Wehring and M. E. Wyman, *Phys. Rev.* **157**, 1803 (1967).

^dV. V. Sklyarevskii, E. P. Stepanov, and B. A. Medvedev, *Zh. Eksperim. i Teor. Fiz.* **36**, 326 (1959) [transl.: *Soviet Phys.-JETP* **9**, 225 (1959)]. Normalization based on Ref. e.

^eV. V. Sklyarevskii, D. E. Fomenko, and E. P. Stepanov, *Zh. Eksperim. i Teor. Fiz.* **32**, 256 (1957) [transl.: *Soviet Phys.-JETP* **5**, 220 (1957)].

^fV. K. Voitovetsky, B. A. Levin, and E. V. Marchenko, *Zh. Eksperim. i Teor. Fiz.* **32**, 263 (1957) [transl.: *Soviet Phys.-JETP* **5**, 184 (1957)].

^gP. D. La Fleur and H. C. Griffin, *Inorg. Nucl. Chem. Letters* **5**, 845 (1969).

^hV. P. Eismont and V. A. Yurgenson, *Yadern. Fiz.* **5**, 1192 (1967) [transl.: *Soviet J. Nucl. Phys.* **5**, 852 (1967)].

ⁱS. S. Kapoor, V. S. Ramamurthy, and R. Zaghoul, *Phys. Rev.* **177**, 1776 (1969).

^jM. E. Wyman, private communication. In the case of Ref. c, the effective observation interval was difficult to assess. The communication also reaffirmed the uncertainty of Ref. 9.

TABLE IV. Estimated internal conversion and x-ray yields. Half the observed photon spectrum was assigned to fragments with $Z = 39$, and half to $Z = 55$. A modified trapezoidal quadrature was employed to sum over the data. Conversion coefficients were interpolated from the work of Hager and Seltzer (Ref. a).

	$Z = 39$			$Z = 55$		
	E1	E2	M1	E1	E2	M1
K-shell ^b						
x rays/fission	0.019	0.18	0.035	0.052	0.30	0.22
K-shell						
vacancies/fission	0.029	0.27	0.052	0.059	0.34	0.25
K-shell ^c						
energy/fission						
(keV)	4.1	29.	8.0	9.0	43.	36.
LM ^d primary						
vacancies/fission	0.0037	0.062	0.0066	0.010	0.25	0.04
LM energy/fission						
(keV)	0.5	5.6	1.0	1.4	21.	5.6
Total converted						
energy/fission						
(keV)	4.6	34.	9.0	10.	64.	42.

^aR. W. Hager and E. C. Seltzer, *Nucl. Data* **A4**, 1 (1968).

^bK-shell fluorescent efficiencies $\omega_K = 0.67$ and 0.88 for $Z = 39$ and 55 were obtained from A. H. Wapstra, G. J. Nijgh, and R. Van Lieshout, *Nuclear Spectroscopy Tables* (North-Holland Publishing Company, Amsterdam, The Netherlands, 1959), Chap. 7, p. 81.

^cThe energy/fission dissipated in lieu of a γ ray, including conversion electron, x rays, and Auger electrons.

^dLM \equiv L shell + M shell. Vacancies and converted transition energies are primary, i.e., they do not include the effect of transitions from K-shell vacancies.

choosing an over-all multipole order that performing a careful average over the fragment atomic number seems unnecessary. For ^{235}U nearly all x rays arise from fragments with $Z = 55 \pm 3$ and 39 ± 3 , taking into account that the number of x rays per fragment rises with Z for each fragment group. Over this range the important conversion coefficients vary only 20%, while choices of multipole order affect the result by factors of 2 to 10.

Line one of Table IV shows the x-ray yields estimated using the spectrum of Fig. 5, for energies ≥ 45 keV, weighted by the conversion coefficients⁵⁸ for $Z = 39$ and 55. We assumed that half the gross spectrum is emitted from the light fragments. It is known that the gross γ spectrum is roughly equally divided between light and heavy fragments,¹ although the energy sensitivity of the referenced experiment is obscure so the spectra could differ considerably in the important energy region below 0.5 MeV. Higher multipole orders were omitted from Table IV because they cannot contribute importantly to the prompt radiation. Assuming the values of x-ray yields observed in this experiment, Table IV shows that all pure multipole-order spectra are excluded for the light-fragment group but not for the heavy-fragment group, though 100% deexcitation by $M1$ transitions seems completely implausible. Numerous combinations of multipolarity are consistent with the data, including roughly equal admixtures of $E1$ and $E2$. Recent work with ^{252}Cf (Ref. 5) gives strong independent evidence that $E2$ transitions in strongly excited ground-state rotational bands contribute importantly to fission γ -ray spectra.

F. Comparisons with Theory

The mean gross energy release in photon emission prior to any β decay is the quantity usually estimated in theoretical studies of the deexcitation of the ensemble of possible fission fragments. Therefore, for comparison purposes one should add to the observed 7.25 MeV/fission the estimated contributions from delayed photon emission from isomeric states as well as the energy dissipated in conversion electrons. Based on Table I of Ref. 12, the energy release per fission from delayed radiation out to a few microseconds is estimated to be 180 ± 50 keV. Table II of Ref. 10 implies that isomers studied in the region 50 μsec to 1 msec account for about 44 keV/fission. Allowing for the unstudied time region and for internal conversion of isomeric transitions leads to an over-all estimate for the delayed photon component of perhaps 350 ± 100 keV. The average electron-converted transition energies of Table IV, choosing any multipole combination which fits the yields,

leads to an estimate of 45 ± 20 keV as the energy/fission emitted in conversion and Auger electrons and in L x rays. The corrected experimental value of the total " γ deexcitation energy" becomes 7.65 ± 0.28 MeV/fission.

To predict the photon energy release (or the spectrum) from theory, it is necessary to judge the multivariate Z , A , and excitation-energy distribution of the ensemble of the photon-emitting fragments. An estimate of this distribution can be based on knowledge gained in many differential multiparameter studies of the fragment energies, velocities, and neutron-emission properties. With these one must employ an empirical mass formula valid far from the stability line and a method for estimating the competition between neutron and photon emission for fragments having excitation energies not far above their neutron-emission thresholds. The method may be constrained to give correctly the prompt neutron multiplicity and energy release. No completely satisfactory solution for this problem has been presented, though the empirical data on which to base the (Z, A, E^*) distribution has gradually been refined since the first estimates of the photon yield were generated. Even with the present state of the data, however, a number of assumptions are required.

Estimators of photon energy release have used various approximations to simplify the handling of the fragment ensemble; all the earlier authors assumed that neutron evaporation proceeds when energetically possible. In no case does the calculated photon energy release include any contribution (or energy dissipation) from processes conceptually preceding the separation of the fragments. The paragraphs below review the published estimates. As detailed knowledge of the input data has developed, a larger electromagnetic energy release has been predicted.

Leachman²⁰ used the isobar mass-parabola parameters of Coryell,⁵⁹ three mass ratios, and fixed Z values to represent the fragment ensemble, and took the excitation-energy distributions of heavy and light fragments as independent and equal. He obtained a photon energy release of 3.8 MeV.

Terrell⁶⁰ obtained about 6.7 MeV if he applied an extremely simplified deexcitation model which assumed a fixed sum for neutron separation plus kinetic energies at each stage in the neutron evaporation process. This simple model, with normal excitation-energy density functions, was adequate to explain the distribution of neutron multiplicities. A later estimate by Terrell²¹ was based on a fixed neutron binding energy of 5.4 MeV though the author recognized that the binding energy tends to rise as successive evaporations occur. The same distribution of excitation energies was employed

along with the usual assumption of nuclear temperature proportional to the square-root of the residual excitation, and the photon energy release was computed as $\sim 0.9 \times$ (average neutron separation energy) regardless of the level-density constant or the total excitation energy available. For the assumed mean separation energy of 5.4 MeV, Terrell's estimated release was about 4.9 MeV/fission. Since Terrell's estimates were based on analyses which sought to elucidate and interrelate the simplest results of fission energetics and evaporation theory, one should not expect his estimates to be more reliable than those of Leachman.

With the idea of obtaining a match to observed radiochemical yields by starting from velocity and kinetic energy data on initial mass distributions, Ferguson and Read²² performed calculations which assumed the mass formulation of Cameron⁶¹ and allowed the parameters of the excitation-energy distribution to vary with fragment mass, so that the average neutron multiplicity vs mass could be fit. However, to make the effort tractable, all neutrons were taken to be emitted with a fixed energy (1.21 MeV) in the fragment reference frame. This approximation can be assumed to have biased the results, but perhaps not enough to account for the 1.4-MeV/fission photon energy release which was obtained.

ZSP⁹ were apparently the first to perform a full average over the fragment mass distribution, employing the standard evaporation theory with a fixed A dependence of the level density parameter, the Cameron mass formulation,⁶¹ and other empirical data on the fragment ensemble. The results for neutron emission are not described. A photon energy release of 5.9 MeV was obtained, almost equally divided between the light and heavy fragments, if photon emission was not allowed to compete with neutron emission. An upper limit of an additional 0.3-MeV additional photon energy was estimated to be obtainable by permitting competition between neutron emission and electric dipole photon emission. (This paper reports that the average binding energy of a neutron in a fission fragment turned out to be 6.25 MeV; given these data, Terrell's 1959 estimated photon energy release would have been 5.7 MeV/fission.) ZSP also estimated the spectrum of the prompt photons on the basis of cascades of electric dipole transitions. The results are compared with the results of this experiment in Fig. 5. The agreement with the measured distribution between 1.5 and 4 MeV is good. ZSP remark that the distribution of excitation energies given by the statistical theory led to a larger fraction of low excitations than seems physically justified considering the small level densities actually observed near the ground states of nu-

clides in this mass region.

Gordon and Aras²⁴ used Monte Carlo evaporation techniques to examine the neutron spectrum and photon energy release from ²³⁵U fission. The mass relation of Seeger⁶² was employed. This calculation did not allow any neutron emission to leave the residual nucleus with less excitation than the pairing-energy correction δ used to improve the level-density estimates for even N and/or Z . A photon energy release consistent with experiment (7.66 MeV/fission) was estimated in this way, while only 5 MeV was obtained if the pairing corrections were set to zero. (Distortions of the Z dependence of the independent yields also seemed to occur if the pairing energy was ignored.) Such corrections for pairing energy are logically used in evaluating competition between decay modes; but, as suggested by Gordon and Aras²⁴ and by Dostrovsky,⁶³ seem artificial when employed to entirely inhibit evaporation.

Thomas and Grover²³ investigated the effect of the spin of the fragments upon the competition between neutron and photon emission, choosing a distribution of fragment spins having a mean value $\sim 5\hbar$ based on radiochemical observations of relative isomer yields. Fragments of ⁹⁶Sr and ¹⁴⁰Xe were chosen to represent the light- and heavy-fragment distributions. Mean excitation energies were chosen to account for the observed number of neutrons emitted in this mass range, with neutron separation energies based on Seeger's tables, plus the photon energy release known to occur. The purpose was to determine whether, given a reasonable excitation-energy distribution, the competition between photon and neutron decay could be handled correctly by taking into account that below a certain excitation energy (the "yrast" level), levels do not occur with a given spin. Neutron emission with low orbital angular momentum is inhibited until the excitation energy is above the neutron-emission threshold for excitation of the appropriate yrast level. The computed mean photon energy release was about 7.1 MeV/fission with an average photon energy of 0.87. The computed mean energy release from the heavy fragment group dropped from 3.1 to 2.0 MeV/fission when the fragment spin was ignored in an otherwise similar computation. The results confirm that the fragment spin effect (with the chosen initial spin) has the correct general magnitude to explain why more detailed estimates ignoring this effect yielded too little photon energy. The spectrum estimated by Grover and Thomas²³ is similar in shape to that observed, gradually falling below the observations at energies above 3 MeV. Fragment spin should be taken into account in a comprehensive computation averaging the emitted photon

spectrum over the whole fragment ensemble using excitation energies based on observed kinetic energy distributions, but the uncertainties in the spin distribution, the mass equation,⁶⁵ and the other input quantities may make the slightly circular method of Thomas and Grover a most appropriate one for demonstrating the fragment-spin effect.

The idea is in question that a variety of fission data requires high average spin for the initial fragments. For example, the photon spectrum of ZSP,¹⁹ predicted without regard for fragment spin, resembles the data closely enough that the nearly exponential gross shape cannot require special properties of the initial spin distribution, unless the more negative slope below 1.5 MeV is the significant feature. Also, though the Kapoor and Ramana analysis of fragment-photon angular correlation did imply very high initial spins,³ Hoffman's analysis of very similar experimental results indicated that spins of $(6-7)\hbar$ are needed for only 20% of the fragments.³³

With mass formulas which have been employed, the observed photon energy release per fission can be predicted only if photon decay competes favorably with neutron decay for fragment excitation energies up to an average of 1 or 1.5 MeV above the neutron-emission threshold. The favored explanation of this finding depends on having high average spins for the initial fission fragments, but evidence from the shape of the spectrum and the γ -

ray angular correlation does not now assure these high spins.

V. ACKNOWLEDGMENTS

The authors acknowledge the essential contributions of the associated authors: T. A. Love participated in all aspects of instrument development, source-strength determinations, and in obtaining the experimental data; R. O. Chester developed the nonlinear fitting programs and fitting functions used to parametrize the spectrometer responses, and applied these to the calibration data; and W. Zobel carried out the actual spectrometer response-function generation and spectral data unfolding. The unfolding was made possible by use of the FERD method of W. R. Burrus, who freely gave advice concerning its wise use. The late R. D. Smidde tested, maintained, and helped improve the electronic equipment. The entire staff of the Bulk Shielding Facility helped make possible the long experimental runs.

R. K. Abele and his group provided fission chambers and advice on their use, while the spectrometer mechanical designs were furnished by H. J. Stripling, R. L. Simpson, T. F. Sliski, and the late F. R. Duncan. W. L. Lyon provided analyses of the contents of the fission chambers and consultation concerning the ionization chambers used in source-strength determinations.

*Final analysis sponsored by the Los Alamos Scientific Laboratory of the U. S. Atomic Energy Commission.

†Joined by T. A. Love particularly for the experimental work, by R. O. Chester for characterization of the response functions, and by W. Zobel for unscrambling the photon spectrum from the pulse-height spectrum.

‡Operated by Union Carbide Corporation under contract with the U. S. Atomic Energy Commission.

¹S. A. E. Johansson and P. Kleinheinz, in *Alpha-, Beta-, and Gamma-Ray Spectroscopy*, edited by K. Siegbahn (North-Holland Publishing Company, Amsterdam, The Netherlands, 1965), Vol. I, Chap. 14, p. 805. See also S. A. E. Johansson, Nucl. Phys. **60**, 378 (1964).

²H. Maier-Leibnitz *et al.*, in *Proceedings of the Symposium on the Physics and Chemistry of Fission, Salzburg, Austria, 1965* (International Atomic Energy Agency, Vienna, Austria, 1965), Vol. II, p. 113; see also H. Maier-Leibnitz, H. W. Schmitt, and P. Armbruster, *ibid.*, p. 143.

³S. S. Kapoor and R. Ramanna, Phys. Rev. **133**, B598 (1964).

⁴G. V. Val'skii, D. M. Kaminker, G. A. Petrov, and L. A. Popeko, At. Energ. (USSR) **18**, 223 (1965) [transl.: Soviet J. At. Energ. **18**, 279 (1965)].

⁵E. Cheifetz, R. C. Jared, S. G. Thompson, and J. B. Wilhelmy, Phys. Rev. Letters **25**, 38 (1970).

⁶K. L. Wolf, R. Vandenbosch, P. A. Russo, M. K.

Mehta, and C. R. Rudy, Phys. Rev. C **1**, 2096 (1970).

⁷U. Stavinski and M. O. Shaker, Nucl. Phys. **62**, 667 (1965). This paper implies that if the thermal-neutron fission cross section of ²³⁵U arises from a 4⁻ resonance, a much higher fraction of the reactions must be of the (*n*, γ f) variety. See also J. D. Garrison, Gulf General Atomic Report No. GA-9141, 1968 (unpublished).

⁸J. E. Lynn, *The Theory of Neutron Resonance Reactions* (Clarendon Press, Oxford, England, 1968), p. 432; see also J. E. Lynn, Phys. Letters **18**, 31 (1965).

⁹L. Bridwell, M. E. Wyman, and B. W. Wehring, Phys. Rev. **145**, 963 (1966).

¹⁰R. E. Sund and R. B. Walton, Phys. Rev. **146**, 824 (1966).

¹¹S. A. E. Johansson, Nucl. Phys. **64**, 147 (1965).

¹²F. C. Maienschein *et al.*, in *Proceedings of the Second United Nations International Conference on Peaceful Uses of Atomic Energy, Geneva, Switzerland, 1958* (United Nations, Geneva, Switzerland, 1958), Vol. 15, p. 366; R. W. Peelle *et al.*, in *Proceedings of the Symposium on Pile Neutron Research in Physics, Vienna, Austria, 1962* (International Atomic Energy Agency, Vienna, Austria, 1962), p. 273.

¹³F. C. Maienschein, *Engineering Compendium on Radiation Shielding* (Springer-Verlag, Inc., New York, 1968), Vol. I, p. 77.

¹⁴J. E. Francis and R. L. Gamble, Oak Ridge National

- Laboratory Report No. ORNL-1879, 1955 (unpublished), p. 20; R. L. Gamble, Ph. D. thesis, University of Texas, 1955 (unpublished).
- ¹⁵V. F. E. W. Rau, *Ann. Physik* **10**, 252 (1963). A plot of Rau's results in Ref. 2, p. 115, when compared with the plots in Ref. 25 which compare the present work with that of Ref. 12, indicates that Rau's results do not clearly support the 9.5-MeV/fission integral which he quotes. The 9.5-MeV estimate was apparently based on the number of observed saturated pulses together with an average energy/photon from Ref. 12 for photons of energy >2.5 MeV. His spectral results plotted in Ref. 2 fall below those of Ref. 12 at energies below 0.6 MeV, as do the results presented here.
- ¹⁶V. V. Verbinski and R. E. Sund, Defense Atomic Support Agency Report No. DASA 2234 (GA-9148), 1969 (unpublished).
- ¹⁷A. E. Smith, P. R. Fields, and A. M. Friedman, *Phys. Rev.* **104**, 699 (1956).
- ¹⁸H. R. Bowman and S. G. Thompson, in *Proceedings of the Second United Nations International Conference on Peaceful Uses of Atomic Energy, Geneva, Switzerland, 1958* (United Nations, Geneva, Switzerland, 1958), Vol. 15, p. 212.
- ¹⁹V. P. Zommer, A. E. Savel'ev, and A. I. Prokofiev, *Soviet J. At. Energy* **19**, 1004 (1965); and also *J. Nucl. Energy Pt. A, B* **20**, 881 (1966).
- ²⁰R. B. Leachman, *Phys. Rev.* **101**, 1005 (1956).
- ²¹J. Terrell, *Phys. Rev.* **113**, 527 (1959).
- ²²J. M. Ferguson and P. A. Read, *Phys. Rev.* **139**, B56 (1965).
- ²³T. D. Thomas and J. R. Grover, *Phys. Rev.* **159**, 980 (1967).
- ²⁴G. E. Gordon and N. K. Aras, in *Proceedings of the Symposium on the Physics and Chemistry of Fission, Salzburg, Austria, 1965* (International Atomic Energy Agency, Vienna, Austria, 1965), Vol. II, p. 73; also H. Nakahara, J. W. Harvey, and G. E. Gordon, *Can. J. Phys.* **47**, 2382 (1969).
- ²⁵R. W. Peelle and F. C. Maienschein, Oak Ridge National Laboratory Report No. ORNL-4457, 1970 (unpublished).
- ²⁶R. W. Peelle and F. C. Maienschein, *Nucl. Sci. Eng.* **40**, 485 (1970).
- ²⁷T. H. Braid, in *Scintillation Spectroscopy of Gamma Radiation*, edited by S. M. Shafroth (Gordon and Breach Science Publishers, New York, 1967), Chap. V; S. A. E. Johansson, *Nature* **166**, 794 (1960); and J. K. Bair and F. C. Maienschein, *Rev. Sci. Instr.* **22**, 343 (1951).
- ²⁸E. G. Silver, Oak Ridge National Laboratory Report No. ORNL-2018, 1956 (unpublished), p. 39.
- ²⁹B. Rossi and H. H. Staub, *Ionization Chambers and Counters* (McGraw-Hill Book Company, Inc., New York, 1949), p. 210; and Oak Ridge National Laboratory Instrumentation and Controls Drawing Q-1534.
- ³⁰T. A. Love, W. R. Burrus, and R. W. Peelle, Oak Ridge National Laboratory Report No. ORNL-2609, 1958 (unpublished), p. 135.
- ³¹E. Fairstein, *Rev. Sci. Instr.* **27**, 475 (1956).
- ³²R. W. Peelle and T. A. Love, Oak Ridge National Laboratory Report No. ORNL-2389, 1957 (unpublished), p. 249.
- ³³M. Hoffman, *Phys. Rev.* **133**, B714 (1964); S. Desi *et al.*, *Phys. Letters* **3**, 343 (1963).
- ³⁴R. W. Schumann and J. P. McMahon, *Rev. Sci. Instr.* **27**, 675 (1956).
- ³⁵R. W. Peelle and T. A. Love, Oak Ridge National Laboratory Report No. ORNL-4118, 1967 (unpublished).
- ³⁶T. A. Love, F. C. Maienschein, and R. W. Peelle, Oak Ridge National Laboratory Report No. ORNL-2842, 1959 (unpublished), p. 93.
- ³⁷F. C. Maienschein, R. W. Peelle, and T. A. Love, Oak Ridge National Laboratory Report No. ORNL-2389, 1957 (unpublished), p. 99.
- ³⁸R. W. Peelle, *Nucl. Instr. Methods* **29**, 293 (1964).
- ³⁹F. C. Maienschein and R. W. Peelle, Oak Ridge National Laboratory Report No. ORNL-3016, 1960 (unpublished), p. 82.
- ⁴⁰R. W. Peelle and F. C. Maienschein, Oak Ridge National Laboratory Report No. ORNL-3016, 1960 (unpublished), p. 96.
- ⁴¹L. P. Remsberg, *Ann. Rev. Nucl. Sci.* **17**, 369 (1967).
- ⁴²K. P. Meyer, P. Schmid, and P. Huber, *Helv. Phys. Acta* **32**, 423 (1959).
- ⁴³R. W. Peelle, Oak Ridge National Laboratory Report No. ORNL-CF-61-4-32, 1961 (unpublished).
- ⁴⁴R. B. Roof, Jr., *Phys. Rev.* **113**, 822 (1959).
- ⁴⁵G. W. Grodstein, *Natl. Bur. Std. (U.S.), Circ. No.* **583** (1957).
- ⁴⁶R. O. Chester, R. W. Peelle, and F. C. Maienschein, National Science Series of the National Research Council Committee on Nuclear Science Report No. NAS-NS-3107, 1963 (unpublished), p. 201.
- ⁴⁷P. V. C. Hough, *Phys. Rev.* **73**, 266 (1948).
- ⁴⁸H. West, *Phys. Rev.* **101**, 915 (1960).
- ⁴⁹W. R. Burrus and V. V. Verbinski, *Nucl. Instr. Methods* **67**, 188 (1969) contains a good description of FERDOR, the predecessor of the FERD system. This reference covers the main numerical methods but not the estimate of the FERD confidence interval. [The quantity (τ^2/NC) in this reference is set to unity in FERD.]
- ⁵⁰Half of any dipole transitions of 45 keV would survive the competition with internal conversion and perhaps 0.1 of any $E2$ transitions. (In any case 45-keV $E2$ transitions would require enhancement by ~ 100 to have most of their decay within the 69-nsec coincidence resolving time.) Furthermore, at the ~ 20 keV midpoint between the x-ray peaks the dipole internal conversion coefficients would be 3-10 times as great as at 45 keV, while the observed background seems constant. This experiment does not eliminate the possibility of a weak ($\sim 10\%$) nuclear γ -ray contribution in this energy region.
- ⁵¹If the standard count vector had been employed for the region below 44 keV, the number of photons/fission in the 21- to 44-keV region would have been estimated from FERD outputs as 0.28 ± 0.04 ; and in the 10- to 21-keV region, 0.28 ± 0.10 . These uncertainties do not contain any contribution from uncertainties in the response functions at very low pulse heights.
- ⁵²E. M. Bohn, B. W. Wehring, and M. E. Wyman, *Phys. Rev.* **188**, 1909 (1969).
- ⁵³F. Horsch and W. Michaelis, in *Proceedings of Second Symposium on Physics and Chemistry of Fission, Vienna, Austria, 1969* (International Atomic Energy Agency, Vienna, Austria, 1969), p. 527.
- ⁵⁴L. E. Glendenin, J. P. Unik, and H. C. Griffin, in *Proceedings of the Symposium on the Physics and Chemistry of Fission, Salzburg, Austria, 1965* (International Atomic Energy Agency, Vienna, Austria, 1965), p. 369 or *Phys. Rev.* **140**, 301 (1965).
- ⁵⁵T. D. Thomas *et al.*, in *Proceedings of the Symposium*

on the *Physics and Chemistry of Fission, Salzburg, Austria, 1965* (International Atomic Energy Agency, Vienna, Austria, 1965), p. 385.

⁵⁶W. John, F. W. Guy, and J. J. Wesolowski, University of California Lawrence Radiation Laboratory Report No. UCRL-72501, also *Phys. Rev. C* **2**, 1451 (1970).

⁵⁷L. E. Glendenin and H. C. Griffin, *Phys. Letters* **15**, 153 (1965).

⁵⁸R. S. Hager and E. C. Seltzer, *Nucl. Data* **A4**, 1 (1968).

⁵⁹C. D. Coryell, *Ann. Rev. Nucl. Sci.* **2**, 304 (1953).

⁶⁰J. Terrell, *Phys. Rev.* **108**, 783 (1957). The photon energy release derivable from the method of this paper is given explicitly in Ref. 21.

⁶¹A. W. Cameron, *Can. J. Phys.* **35**, 1021 (1957).

⁶²P. A. Seeger, *Nucl. Phys.* **25**, 1 (1961).

⁶³I. Dostrovsky, Z. Fraenkel, and G. Friedlander, *Phys. Rev.* **116**, 683 (1959).

⁶⁴J. R. Grover and T. D. Thomas, in *American Chemical Society Symposium on Recent Advances in Nuclear Science and Engineering Education*, March 1966, Pittsburgh, Pennsylvania (unpublished); also J. R. Grover, private communication. This work gave additional results from the effort reported in Ref. 23.

⁶⁵For example, Seeger (Ref. 62) reported that his mass formula gives a 0.75-MeV standard deviation with the input odd-*A* masses, and his paper shows a systematic ~ 1 -MeV error near mass 100. Initial fission fragments are away from the valley of β -ray stability, so lacking a published assessment of extrapolation uncertainties, one might expect systematic errors $\gtrsim 1$ MeV/fragment in estimated initial excitation energy.

Energy Levels in Cf²⁵¹ via Alpha Decay of Fm²⁵⁵†

I. Ahmad, F. T. Porter, M. S. Freedman, R. F. Barnes, R. K. Sjoblom, F. Wagner, Jr., J. Milsted, and P. R. Fields

Chemistry Division, Argonne National Laboratory, Argonne, Illinois 60439

(Received 18 August 1970)

The γ -singles and conversion-electron spectra of Fm²⁵⁵ were measured with a Ge(Li) diode and the Argonne double toroidal β -ray spectrometer, respectively. In the γ -ray spectra, in addition to the transitions expected from previously known decay schemes, γ rays of energies 63.8, 131.0, 204.1, and 264.1 keV were observed. Two new α groups, α_{368} (6.765 MeV) and α_{433} (6.701 MeV), were identified in coincidence with 131.0- and 204.1-keV γ rays. A two-parameter γ - γ coincidence experiment showed that the 204.1- and 131.0-keV transitions populate the $\frac{9}{2}^-$ and $\frac{11}{2}^-$ members of the favored band. Conversion-electron studies and α -vs- γ intensity comparisons demonstrate their *E1* character. The half-life of the 370.4-keV level was measured by a delayed α - γ coincidence method and found to be 1.3 ± 0.1 μ sec. On the basis of these observations and the α intensities to these levels, the 370.4- and 434.2-keV levels have been assigned to the $\frac{11}{2}^-$ -(725 \dagger) and $\frac{9}{2}^-$ -(734 \dagger) Nilsson states, respectively. A three-parameter α - γ -time coincidence experiment indicates that the α intensity to the 105.73-keV ($I = \frac{1}{2}$, $K = \frac{1}{2}$) level is less than 1%, implying that its 18% population comes primarily via a 0.57-keV transition from the 106.30-keV, $I = \frac{1}{2}$, $K = \frac{1}{2}$ level. The α transition probabilities to various bands are in agreement with the values expected from α -decay systematics and theoretical calculations. The *K*-, *L*-, *M*-, and *N*-sunshell atomic electron binding energies in Cf ($Z = 98$), obtained experimentally by least-squares adjustment from the conversion-line data, show significant deviations below recent (Bearden and Burr) tabulated values.

I. INTRODUCTION

The decay scheme of Fm²⁵⁵ was first investigated by Asaro, Bjørnholm, and Perlman (ABP).¹ The ground state and the level at 106 keV in Cf²⁵¹ were given the Nilsson-state² assignments of $\frac{1}{2}^+$ -(620 \dagger) and $\frac{7}{2}^+$ -(613 \dagger), respectively. These assignments are based on the observed rotational level spacings, intensity patterns, and the multipolarities of prominent interband transitions. γ - α and electron- α coincidence measurements showed the existence of another level at 546 keV (α intensity = 0.05%) which decays via a 426-keV level to the 106-keV

state. The 426- and 546-keV levels were given the tentative assignments of $\frac{9}{2}^+$ -(615 \dagger) and $\frac{11}{2}^-$ -(725 \dagger), respectively. Later work by Ahmad³ showed that the α spectrum measured in coincidence with γ rays is very complex, and the above assignments of the 426- and 546-keV levels are not correct. From his coincidence measurements, he was able to identify two new rotational bands with band-head energies at 178 and 550 keV, and assigned them to the $\frac{3}{2}^+$ -(622 \dagger) and $\frac{5}{2}^+$ -(622 \dagger) neutron states, respectively. A decay scheme representing a composite of the results obtained by ABP and Ahmad³ is shown in Fig. 1. A recent study⁴ of the electron